J Mol Model (2012) 18:4477–4489
DOI 10.1007/s00894-012-1440-1

ORIGINAL PAPER

Electric field effect on (6,0) *zigzag* single-walled aluminum nitride nanotube

Mohammad T. Baei · Ali Ahmadi Peyghan · Masoumeh Moghimi

Received: 27 February 2012 / Accepted: 18 April 2012 / Published online: 29 May 2012

Abstract Structural, electronic, and electrical responses of the H-capped (6,0) *zigzag* single-walled aluminum nitride nanotube was studied under the parallel and transverse electric fields with strengths $0–140\times10^{-4}$ a.u. by using density functional calculations. Geometry optimizations were carried out at the B3LYP/6-31G* level of theory using a locally modified version of the GAMESS electronic structure program. The dipole moments, atomic charge variations, and total energy of the (6,0) *zigzag* AlNNT show increases with increase in the applied external electric field strengths. The length, tip diameters, electronic spatial extent, and molecular volume of the nanotube do not significantly change with increasing electric field strength. The energy gap of the nanotube decreases with increases of the electric field strength and its reactivity is increased. Increase of the ionization potential, electron affinity, chemical potential, electrophilicity, and HOMO and LUMO in the nanotube with increase of the applied parallel electric field strengths shows that the parallel field has a much stronger interaction with the nanotube with respect to the transverse electric field strengths. Analysis of the parameters indicates that the properties of AlNNTs can be controlled by the proper external electric field.

Keywords Aluminum nitride nanotube · Dipole moment · External electric field effect · Quantum molecular descriptors · NBO

M. T. Baei (✉)
Department of Chemistry, Azadshahr Branch,
Islamic Azad University,
Azadshahr, Golestan, Iran
e-mail: Baei52@yahoo.com

A. A. Peyghan
Young Researchers Club, Islamshahr Branch,
Islamic Azad University,
Tehran, Iran

M. Moghimi
Department of Chemistry, Gonbad Kavoos Branch,
Islamic Azad University,
Gonbad Kavoos, Golestan, Iran

Introduction

Since the synthesis of carbon nanotubes (CNTs) by Ijima in 1991 [1], single-walled carbon nanotubes (SWCNTs) have attracted great interest owing to their physical and chemical properties [1–3] and applications as novel materials [4, 5]. The electronic properties of CNTs depend on their tubular diameter and chirality. Many investigations have been undertaken to investigate non-carbon-based nanotubes, which exhibit electronic properties independent of these features. Among these, aluminum nitride nanotubes (AlNNTs), which are made from group III and V elements, which are neighbors of carbon in the periodic table, are an interesting subject of many studies [6, 7]. Aluminum nitride nanotubes are inorganic analogs of carbon nanotubes (CNTs) and always behave as semiconductors [6, 7]. Because of their high temperature stability, largest band gap, thermal conductivity, and low thermal expansion [8–10] aluminum nitride (AlN) nonmaterials are widely used in technological applications, mainly in micro and optoelectronics, such as laser diodes and solar-blind ultraviolet photodetectors and semiconductors [10]. Tuning the electronic structures of the semiconducting AlNNTs for specific application is evidently important in building specific electronic and mechanical devices. Improving the sensing performance of the pristine nanotubes and nano sheets by manipulating their structure is too expensive; therefore, finding highly sensitive pristine nanotubes is of scientific interest. Electric field effect is one of the best techniques for improvement of the electronic structure properties of nanotubes and adsorption of gaseous molecules on the tubes surface. In recent years, several studies have studied the computational calculation of the field effects on the electronic and structural properties of nanotubes [11–13]. Machado et al. have investigated on zigzag and armchair single-walled aluminum nitride nanotubes in various diameters under influence of just perpendicular external electric fields in 0.3 and 0.5 V/Å. They showed that tubes with larger diameters are more stable and the applied perpendicular external electric fields do not have significant influence on the stability of these structures [14]. However, to our knowledge, no experiments and theoretical investigation have been reported on (6,0) *zigzag* AlNNT surfaces under both parallel and perpendicular static external electric fields, so further study of the electronic properties of aluminum nitride nanotubes remains interesting. The objective of the present work is to study the results of density functional calculations on the geometric and electronic properties of the (6,0) *zigzag* AlNNT, especially charge density distributions, electric dipole moments, molecular orbital energy analysis, energies, molecular volume, density of states, electronic spatial extent (*ESE*), quantum molecular descriptors [15, 16] including electronic chemical potential (μ), global hardness (η), electrophilicity index (ω) [17], energy gap ($E_{HOMO} - E_{LUMO}$), global softness (S), and electronegativity (χ) of the nanotube under the influence both parallel and perpendicular static external electric fields.

Computational methods

In the present work, we studied influence of the static external electric field on structural and electronic properties of the (6,0) *zigzag* AlNNT, separately applied at the positive X- and positive Y-directions, which is parallel and perpendicular to X and Y plane (Fig. 1). Due to the absence of periodic boundary conditions in molecular calculations, it was necessary to saturate the Al and N dangling bonds with H atoms. The hydrogenated model of the pristine (6,0) *zigzag* AlNNT consist of 72 atoms with formula $Al_{30}N_{30}H_{12}$. In the first step, the atomic geometrical parameters of the structure was allowed to relax in the optimization at the DFT level of B3LYP exchange functional and 6-31G* standard basis set. Then, influence of the external electric field at various applied parallel and transverse electric field strengths on the nanotube was studied. The numerical values of the external static electric field strengths in X and Y directions on the (6,0) AlNNT model are 35×10^{-4}, 70×10^{-4}, 100×10^{-4}, and 140×10^{-4} a.u. (1 a.u. = 5.14224×10^{11} V/m) [18].

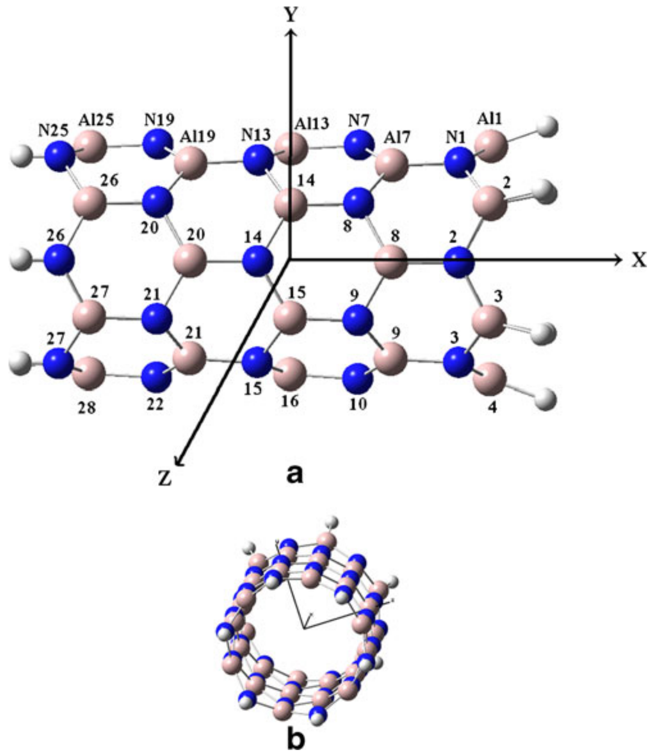

Fig. 1 (**a**) Two-dimensional (2D) and (**b**) Three-dimensional (3D) views of the (6,0) *zigzag* AlNNT

The structural and electronic properties were based on the Al–N bond lengths, bond angles, length of tube, tip diameters, molecular volume, dipole moments (μ), energy gaps, energies, atomic charges, molecular orbital energies, electronic spatial extent (*ESE*), density of states, and quantum molecular descriptors for the nanotube in the above electric fields with X and Y orientations. For the nanotube, the quantum molecular descriptors [15, 16] including electronic chemical potential (μ), global hardness (η), electrophilicity index (ω) [17], energy gap, global softness (S), and electronegativity (χ) of the nanotube was calculated as follows:

$$[\mu = -\chi = -(\mathrm{I} + \mathrm{A})/2] \tag{1}$$

$$[\eta = (\mathrm{I} - \mathrm{A})/2] \tag{2}$$

$$[\omega = \mu^2/2\eta] \tag{3}$$

$$[\mathrm{S} = 1/2\eta], \tag{4}$$

where I ($-E_{HOMO}$) is the first vertical ionization energy and A ($-E_{LUMO}$) the electron affinity of the molecule. The electrophilicity index is a measure of electrophilic power of a molecule. When two molecules react with each other, one molecule behaves as a nucleophile while the other acts as an

Table 1 Optimized bond lengths (Å), bond angles (°), diameters (Å), length of tube (Å), and molecular volume (cm^3 mol^{-1}) of the (6,0) *zigzag* AlNNT at different applied parallel and transverse electric field strengths

Bond length	(6,0) *zigzag* AlNNT									
	X					Y				
	0	35	70	100	140	0	35	70	100	140
Al1-N1	1.817	1.823	1.813	1.811	1.810	1.817	1.825	1.833	1.839	1.849
Al2-N1	1.818	1.813	1.818	1.818	1.820	1.818	1.811	1.805	1.800	1.795
Al2-N2	1.817	1.819	1.803	1.798	1.791	1.817	1.820	1.823	1.826	1.831
Al3-N2	1.817	1.819	1.825	1.828	1.833	1.817	1.817	1.817	1.816	1.816
Al3-N3	1.818	1.813	1.803	1.797	1.789	1.818	1.814	1.811	1.808	1.804
Al4-N3	1.817	1.823	1.821	1.823	1.826	1.817	1.823	1.828	1.833	1.841
Al7-N1	1.814	1.815	1.829	1.836	1.847	1.814	1.815	1.815	1.816	1.817
Al8-N2	1.814	1.816	1.827	1.832	1.840	1.814	1.816	1.819	1.821	1.825
Al9-N3	1.814	1.815	1.822	1.827	1.832	1.814	1.816	1.817	1.819	1.821
Al7-N7	1.815	1.809	1.811	1.810	1.809	1.815	1.809	1.803	1.798	1.791
Al7-N8	1.815	1.820	1.806	1.802	1.798	1.815	1.820	1.826	1.832	1.840
Al8-N8	1.815	1.813	1.820	1.822	1.825	1.815	1.812	1.809	1.807	1.804
Al8-N9	1.815	1.814	1.800	1.794	1.787	1.815	1.816	1.817	1.819	1.821
Al9-N9	1.815	1.820	1.819	1.821	1.823	1.815	1.819	1.823	1.827	1.833
Al9-N10	1.815	1.809	1.804	1.800	1.795	1.815	1.810	1.805	1.800	1.795
Al13-N7	1.812	1.812	1.826	1.833	1.843	1.812	1.812	1.811	1.798	1.811
Al14-N8	1.812	1.813	1.825	1.831	1.840	1.812	1.813	1.814	1.821	1.816
Al15-N9	1.812	1.813	1.823	1.828	1.835	1.812	1.813	1.815	1.817	1.820
Al16-N10	1.812	1.812	1.821	1.826	1.832	1.812	1.812	1.812	1.813	1.813
Al13-N13	1.818	1.824	1.815	1.814	1.813	1.818	1.824	1.831	1.837	1.845
Al14-N13	1.818	1.815	1.820	1.820	1.822	1.818	1.813	1.808	1.804	1.799
Al14-N14	1.818	1.821	1.805	1.800	1.793	1.818	1.822	1.826	1.83	1.837
Al15-N14	1.818	1.821	1.824	1.826	1.830	1.818	1.819	1.820	1.822	1.824
Al15-N15	1.818	1.815	1.803	1.798	1.790	1.818	1.816	1.814	1.813	1.811
Al16-N15	1.818	1.824	1.817	1.817	1.818	1.818	1.824	1.830	1.836	1.844
Al19-N13	1.811	1.811	1.824	1.830	1.839	1.811	1.811	1.811	1.812	1.812
Al20-N14	1.811	1.812	1.823	1.828	1.836	1.811	1.812	1.813	1.815	1.817
Al21-N15	1.811	1.811	1.821	1.826	1.833	1.811	1.811	1.813	1.813	1.815
Al19-N19	1.816	1.810	1.813	1.812	1.811	1.816	1.810	1.803	1.798	1.791
Al19-N20	1.816	1.822	1.808	1.804	1.800	1.816	1.822	1.829	1.836	1.844
Al20-N20	1.818	1.816	1.822	1.824	1.828	1.818	1.814	1.812	1.811	1.809
Al20-N21	1.818	1.816	1.800	1.794	1.786	1.818	1.818	1.820	1.822	1.825
Al21-N21	1.816	1.822	1.819	1.821	1.824	1.816	1.821	1.826	1.831	1.837
Al21-N22	1.816	1.810	1.803	1.798	1.792	1.816	1.811	1.807	1.803	1.799
Al25-N19	1.807	1.807	1.817	1.822	1.828	1.807	1.807	1.807	1.808	1.808
Al26-N20	1.807	1.807	1.817	1.821	1.828	1.807	1.807	1.808	1.808	1.809
Al27-N21	1.807	1.807	1.817	1.821	1.828	1.807	1.807	1.808	1.809	1.810
Al28-N22	1.807	1.807	1.817	1.822	1.829	1.807	1.807	1.807	1.808	1.809
Al25-N25	1.815	1.822	1.816	1.816	1.817	1.815	1.822	1.830	1.836	1.845
Al26-N25	1.816	1.813	1.821	1.823	1.827	1.816	1.811	1.806	1.802	1.798
Al26-N26	1.816	1.820	1.804	1.799	1.793	1.816	1.821	1.827	1.832	1.841
Al27-N26	1.816	1.820	1.824	1.828	1.833	1.816	1.818	1.820	1.823	1.826
Al27-N27	1.816	1.812	1.800	1.795	1.788	1.816	1.814	1.813	1.813	1.812
Al28-N27	1.815	1.822	1.815	1.816	1.818	1.815	1.822	1.830	1.836	1.846
Average Al-N	1.815	1.815	1.815	1.816	1.818	1.815	1.815	1.816	1.817	1.819

Table 1 (continued)

Bond length	(6,0) *zigzag* AlNNT									
	X					Y				
	0	35	70	100	140	0	35	70	100	140
Al-H	1.582	1.585	1.592	1.607	1.621	1.582	1.586	1.592	1.598	1.608
N-H	1.019	1.019	1.020	1.020	1.022	1.019	1.019	1.020	1.021	1.022
Bond angles										
N1-Al7-N8	119.20	118.42	119.06	118.95	118.78	119.20	118.60	117.82	117.10	116.18
N2-Al8-N9	119.28	119.28	119.98	120.31	120.77	119.28	118.97	118.59	118.24	117.66
N7-Al13-N13	119.20	118.63	118.28	117.87	117.32	119.20	118.61	118.06	117.58	116.95
N8-Al14-N14	119.16	118.87	119.28	119.37	119.51	119.16	118.69	118.23	117.82	117.25
Al14-N14-Al20	117.24	116.82	117.28	117.30	117.36	117.24	116.76	116.21	115.72	115.06
N9-Al15-N14	119.16	118.87	117.61	116.92	115.98	119.16	119.09	118.94	118.80	118.61
N10-Al16-N15	119.20	118.63	118.26	117.84	117.25	119.20	118.62	118.03	117.52	116.81
N20-Al20-N21	118.69	119.03	119.85	120.37	121.07	118.69	119.01	119.34	119.58	119.85
N21-Al27-N27	116.78	117.42	117.02	117.13	117.27	116.78	117.31	117.78	118.19	118.72
Diameters										
(Al-tip)	6.33	6.37	6.37	6.43	6.52	6.33	6.36	6.43	6.53	6.68
(N-tip)	6.43	6.44	6.44	6.46	6.57	6.43	6.43	6.46	6.48	6.54
Length of tube (*l*)	10.67	10.64	10.61	10.59	10.56	10.67	10.66	10.64	10.63	10.62
Molecular volume (*V*)	702.82	686.74	641.25			702.82	714.18	642.48	680.35	681.32

electrophile. Higher electrophilicity index shows higher electrophilic of a molecule. The quantum molecular descriptors were compared in the static external electric fields. All the calculations were carried out using a locally modified version of the GAMESS electronic structure program [19].

Results and discussion

Field effect on the structural parameters

The structural properties consisting of the bond lengths, bond angles, tip diameters, and length of tube for the optimized structure of (6,0) *zigzag* AlNNT at various applied parallel and transverse electric field strengths with the significant changes in the parameters are summarized in Tables 1 and 2. The bond lengths obtained at different applied parallel and transverse electric field strengths with respect to the corresponding values at zero fields (E_X=E_Y=0) indicate that the changes of all Al–N, Al–H, and N–H bond lengths of the (6,0) *zigzag* AlNNT model over the entire range of the applied parallel and transverse electric field strengths are <0.04 Å (Table 2). The most significant change in the bond lengths for the applied parallel electric field is observed for the Al7-N1 that increases gradually from 1.814 Å at the zero field strength (E_X=0) to 1.847 Å at the field strength of 140×10^{-4} a.u. (E_X=140). In transverse applied electric field case, the most significant change is observed for the Al1-N1 that increases gradually from 1.817 Å at the zero field strength (E_Y=0) to 1.849 Å at the field strength of 140×10^{-4} a.u. (E_Y=140). The Al20-N21 and Al19-N19 bonds show a significant reverse trend, increasing with increasing parallel and transverse electric field intensity.

The variations in the values of bond angles for applied parallel and transverse electric field strengths in Table 2 indicate that the maximum deviation of optimized bond angles with respect to the corresponding values at zero electric field (E_X=E_Y=0) at various parallel and transverse electric field strengths are less than 4 °. The most significant change in the bond angles for the applied parallel electric field is observed for the N9-Al15-N14 that decreases gradually from 119. 16 ° at the zero field strength (E_X=0) to 115.98 ° at the field strength of 140×10^{-4} a.u. (E_X=140). In transverse applied electric field case, the most significant change is observed for the N1-Al7-N8 that decreases gradually from 119.20 ° at the zero field strength (E_Y=0) to 116.18 ° at the field strength of 140×10^{-4} a.u. (E_Y=140). The results presented in Tables 1 and 2 indicate that the variations in the values of bond lengths and bond angles for applied parallel and transverse electric field strengths in the (6,0) *zigzag* AlNNT model are negligible.

Length of the AlNNT is an important parameter characterizing its structural response to the applied parallel and transverse electric field in the nano-electronic circuit. The

Table 2 Differential values of optimized bond lengths (Å), bond angles (°), diameters (Å), length of tube (Å), and molecular volume (cm^3 mol^{-1}) of the (6,0) *zigzag* AlNNT at different applied parallel and transverse electric field strengths

ΔBond length	(6,0) *zigzag* AlNNT									
	X					Y				
	0	35	70	100	140	0	35	70	100	140
Al1-N1	0.000	0.006	−0.004	−0.006	−0.007	0.000	0.008	0.016	0.022	0.032
Al2-N1	0.000	−0.005	0.000	0.000	0.002	0.000	−0.007	−0.013	−0.018	−0.023
Al2-N2	0.000	0.002	−0.014	−0.019	−0.026	0.000	0.003	0.006	0.009	0.014
Al3-N2	0.000	0.002	0.008	0.011	0.016	0.000	0.000	0.000	−0.001	−0.001
Al3-N3	0.000	−0.005	−0.015	−0.021	−0.029	0.000	−0.004	−0.007	−0.010	−0.014
Al4-N3	0.000	0.006	0.004	0.006	0.009	0.000	0.006	0.011	0.016	0.024
Al7-N1	0.000	0.001	0.015	0.022	0.033	0.000	0.001	0.001	0.002	0.003
Al8-N2	0.000	0.002	0.013	0.018	0.026	0.000	0.002	0.005	0.007	0.011
Al9-N3	0.000	0.001	0.008	0.013	0.018	0.000	0.002	0.003	0.005	0.007
Al7-N7	0.000	−0.006	−0.004	−0.005	−0.006	0.000	−0.006	−0.012	−0.017	−0.024
Al7-N8	0.000	0.005	−0.009	−0.013	−0.017	0.000	0.005	0.011	0.017	0.025
Al8-N8	0.000	−0.002	0.005	0.007	0.010	0.000	−0.003	−0.006	−0.008	−0.011
Al8-N9	0.000	−0.001	−0.015	−0.021	−0.028	0.000	0.001	0.002	0.004	0.006
Al9-N9	0.000	0.005	0.004	0.006	0.008	0.000	0.004	0.008	0.012	0.018
Al9-N10	0.000	−0.006	−0.011	−0.015	−0.020	0.000	−0.005	−0.010	−0.015	−0.020
Al13-N7	0.000	0.000	0.014	0.021	0.031	0.000	0.000	−0.001	−0.014	−0.001
Al14-N8	0.000	0.001	0.013	0.019	0.028	0.000	0.001	0.002	0.009	0.004
Al15-N9	0.000	0.001	0.011	0.016	0.023	0.000	0.001	0.003	0.005	0.008
Al16-N10	0.000	0.000	0.009	0.014	0.020	0.000	0.000	0.000	0.001	0.001
Al13-N13	0.000	0.006	−0.003	−0.004	−0.005	0.000	0.006	0.013	0.019	0.027
Al14-N13	0.000	−0.003	0.002	0.002	0.004	0.000	−0.005	−0.010	−0.014	−0.019
Al14-N14	0.000	0.003	−0.013	−0.018	−0.025	0.000	0.004	0.008	0.012	0.019
Al15-N14	0.000	0.003	0.006	0.008	0.012	0.000	0.001	0.002	0.004	0.006
Al15-N15	0.000	−0.003	−0.015	−0.020	−0.028	0.000	−0.002	−0.004	−0.005	−0.007
Al16-N15	0.000	0.006	−0.001	−0.001	0.000	0.000	0.006	0.012	0.018	0.026
Al19-N13	0.000	0.000	0.013	0.019	0.028	0.000	0.000	0.000	0.001	0.001
Al20-N14	0.000	0.001	0.012	0.017	0.025	0.000	0.001	0.002	0.004	0.006
Al21-N15	0.000	0.000	0.010	0.015	0.022	0.000	0.000	0.002	0.002	0.004
Al19-N19	0.000	−0.006	−0.003	−0.004	−0.005	0.000	−0.006	−0.013	−0.018	−0.025
Al19-N20	0.000	0.006	−0.008	−0.012	−0.016	0.000	0.006	0.013	0.020	0.028
Al20-N20	0.000	−0.002	0.004	0.006	0.010	0.000	−0.004	−0.006	−0.007	−0.009
Al20-N21	0.000	−0.002	−0.018	−0.024	−0.032	0.000	0.000	0.002	0.004	0.007
Al21-N21	0.000	0.006	0.003	0.005	0.008	0.000	0.005	0.010	0.015	0.021
Al21-N22	0.000	−0.006	−0.013	−0.018	−0.024	0.000	−0.005	−0.009	−0.013	−0.017
Al25-N19	0.000	0.000	0.010	0.015	0.021	0.000	0.000	0.000	0.001	0.001
Al26-N20	0.000	0.000	0.010	0.014	0.021	0.000	0.000	0.001	0.001	0.002
Al27-N21	0.000	0.000	0.010	0.014	0.021	0.000	0.000	0.001	0.002	0.003
Al28-N22	0.000	0.000	0.010	0.015	0.022	0.000	0.000	0.000	0.001	0.002
Al25-N25	0.000	0.007	0.001	0.001	0.002	0.000	0.007	0.015	0.021	0.030
Al26-N25	0.000	−0.003	0.005	0.007	0.011	0.000	−0.005	−0.010	−0.014	−0.018
Al26-N26	0.000	0.004	−0.012	−0.017	−0.023	0.000	0.005	0.011	0.016	0.025
Al27-N26	0.000	0.004	0.008	0.012	0.017	0.000	0.002	0.004	0.007	0.010
Al27-N27	0.000	−0.004	−0.016	−0.021	−0.028	0.000	−0.002	−0.003	−0.003	−0.004
Al28-N27	0.000	0.007	0.000	0.001	0.003	0.000	0.007	0.015	0.021	0.031
Average Al-N	0.000	0.000	0.000	0.001	0.003	0.000	0.000	0.001	0.002	0.004

Table 2 (continued)

ΔBond length	(6,0) *zigzag* AlNNT									
	X					Y				
	0	35	70	100	140	0	35	70	100	140
Al-H	0.000	0.003	0.010	0.025	0.039	0.000	0.004	0.010	0.016	0.026
N-H	0.000	0.000	0.001	0.001	0.003	0.000	0.000	0.001	0.002	0.003
ΔBond angles										
N1-Al7-N8	0.00	−0.78	−0.14	−0.25	−0.42	0.00	−0.60	−1.38	−2.10	−3.02
N2-Al8-N9	0.00	0.00	0.70	1.03	1.49	0.00	−0.31	−0.69	−1.04	−1.62
N7-Al13-N13	0.00	−0.57	−0.92	−1.33	−1.88	0.00	−0.59	−1.14	−1.62	−2.25
N8-Al14-N14	0.00	−0.29	0.12	0.21	0.35	0.00	−0.47	−0.93	−1.34	−1.91
Al14-N14-Al20	0.00	−0.42	0.04	0.06	0.12	0.00	−0.48	−1.03	−1.52	−2.18
N9-Al15-N14	0.00	−0.29	−1.55	−2.24	−3.18	0.00	−0.07	−0.22	−0.36	−0.55
N10-Al16-N15	0.00	−0.57	−0.94	−1.36	−1.95	0.00	−0.58	−1.17	−1.68	−2.39
N20-Al20-N21	0.00	0.34	1.16	1.68	2.38	0.00	0.32	0.65	0.89	1.16
N21-Al27-N27	0.00	0.64	0.24	0.35	0.49	0.00	0.53	1.00	1.41	1.94
ΔDiameters										
(Al-tip)	0.00	0.04	0.04	0.10	0.19	0.00	0.03	0.10	0.20	0.35
(N-tip)	0.00	0.01	0.01	0.03	0.14	0.00	0.00	0.03	0.05	0.11
Length of tube (Δl)	0.00	−0.03	−0.06	−0.08	−0.11	0.00	−0.01	−0.03	−0.04	−0.05
Molecular volume (ΔV)	0.00	−16.08	−61.57			0.00	11.36	−60.34	−22.47	−21.50

distance between the Al2 and Al26 atoms of the AlNNT model (see Fig. 1) considered as the length (l) of the tube. The calculated lengths and tip diameters of the nanotube at various parallel and transverse electric field strengths with respect to the corresponding values at zero field (E_X=E_Y=0) with significant changes in the parameters are presented in Tables 1 and 2. The results indicate that length of the nanotube does not change significantly with increasing electric field strengths from 0–140×10^{-4} a.u. (< 1.03 %). This length resistance of the nanotube against external electric field can be considered as an advantage for the nanotube in molecular scale device. Also, the values of tip diameters of the nanotube increased slightly by external electric field (see Table 2).

Molecular volume is one of the important parameters that reflects the molecular geometric response to the applied parallel and transverse electric field strengths. This parameter is defined as the volume inside a contour of 0.001 electron/bohr^3 density. The calculated molecular volume of the (6,0) *zigzag* AlNNT at various parallel and transverse electric field strength with respect to the corresponding values at zero fields (E_X=E_Y=0) with significant changes in the parameters are presented in Tables 1 and 2. The results presented in the tables indicate that variations of the molecular volume for the applied parallel and transverse electric field strengths do not have any well-defined trend from zero to 140×10^{-4} a.u..

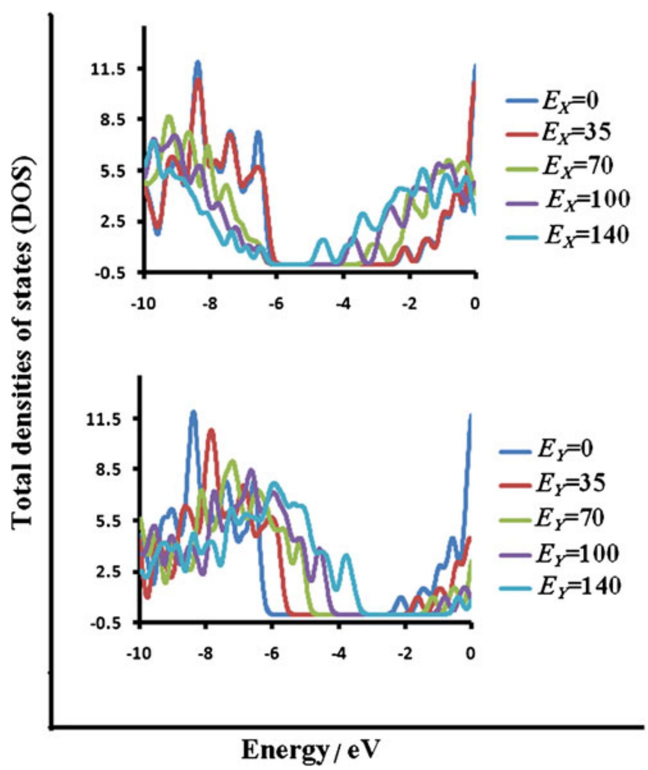

Fig. 2 Total densities of states (DOS) for the (6,0) *zigzag* AlNNT at different applied parallel and transverse electric field strengths

Table 3 Optimized properties of the (6,0) *zigzag* AlNNT at different applied parallel and transverse electric field strengths

Property	(6,0) *zigzag* AlNNT								
	X					Y			
	0	35	70	100	140	35	70	100	140
E_T *AlNNT/keV*	−242.8876	−242.8877	−242.8888	−242.8897	−242.8914	−242.8877	−242.8882	−242.8889	−242.8901
Energy gaps/eV	4.29	4.17	3.37	2.74	1.76	4.17	3.90	3.61	3.15
$ESE/bohr^2=a_0^2$	54954.88	54957.67	54870.71	54851.92	54842.18	54961.37	54965.37	54978.60	55001.84
$\Delta ESE/\ bohr^2=a_0^2$	0.00	2.79	−84.17	−102.96	−112.70	6.49	10.49	23.72	46.96
μ_{Tot}/ *Debye*	12.30	14.88	28.73	36.61	47.42	15.04	21.09	27.39	36.55

Field effect on electronic properties of the (6,0) zigzag AlNNT model

Densities of states (DOS)

We studied the influence of external electric field on the electronic properties of the nanotube. The total densities of states (DOS) of the nanotube at various applied parallel and transverse electric field strengths are shown in Fig. 2. As is evident from Fig. 2 and Table 3, the energy gap obtained from these calculations at different applied parallel and transverse electric field strengths with respect to the corresponding values at zero fields (E_X=E_Y=0) indicate that with increasing parallel and transverse electric field intensity, the energy gap values are decreased. The energy gap value for the applied parallel electric field is gradually decreased from 4.29 eV at the zero field strength (E_X=0) to 1.76 eV at the field strength of 140×10^{-4} a.u. (E_X=140) and the energy gap value for the applied transverse electric field is gradually decreased from 4.29 eV at the zero field strength (E_Y=0) to 3.15 eV at the field strength of 140×10^{-4} a.u. (E_Y=140). The total densities of states (TDOS) of these tubes show significant changes due to external electric field in the gaps regions of the TDOS plots. In comparison with the zero field strength, the energy gaps of the nanotube by external electric field were reduced while their electrical conductance was increased. Also, these results show that the applied parallel electric field has more influence on the energy gap of the nanotube than the applied transverse electric field and easier to modulate by the applied parallel electric field. This trend is in agreement with the changes in the total energy (E_T) of the nanotube, with the applied parallel electric field having a stronger effect on the E_T of the nanotube than the applied transverse electric field (see Table 3).

Electronic spatial extent (ESE)

The electronic spatial extent (ESE) for every nanotube is defined as the surface area covering a volume around the nanotube and describes the gross receptivity of the nanotube from an external electric field. The ESE of the (6,0) zigzag AlNNT at various parallel and transverse electric fields with the significant changes in the parameter are summarized in Table 3. The results indicate that the ESE of the nanotube does not change significantly with increasing electric field strengths from 0–140×10^{-4} a.u. (< 0.2 %). These slight changes of ESE against external electric field can be regarded as a positive index for the nanotube as a nano-device in nano-circuits.

Molecular orbital (MO)

To better understand the electric response and electrical transport in (6,0) AlNNT nanotube, we studied the electronic energies of the nanotube at different applied parallel and transverse electric field strengths, because electric response and electrical transport depend on all the molecular orbital energy spacings between the occupied (HOMO) and virtual (LUMO) molecular orbitals. The highest occupied molecular orbital (HOMO) and lowest unoccupied molecular orbital (LUMO) energies for the nanotube as functions of the different applied parallel, E_X, and perpendicular, E_Y, electric field strengths are plotted in Fig. 3. As is evident from Fig. 3, for parallel case, both the HOMO and LUMO are more stabilized compared with the perpendicular case. The HOMO and LUMO values for the applied parallel electric field is gradually increased from −6.42 and −2.13 eV at the zero field strength (E_X=0) to −6.48 and −4.72 eV at the field strength of 140×10^{-4} a.u. (E_X=140) and the HOMO and

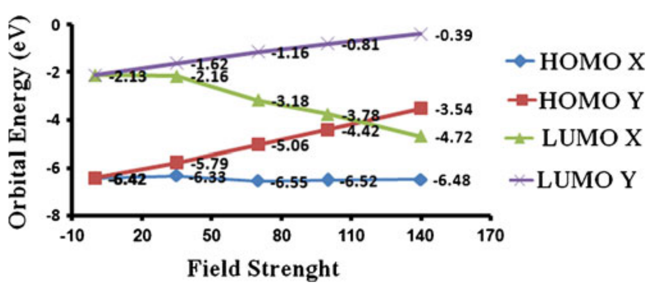

Fig. 3 HOMO and LUMO for the (6,0) *zigzag* AlNNT at different applied parallel and transverse electric field strengths

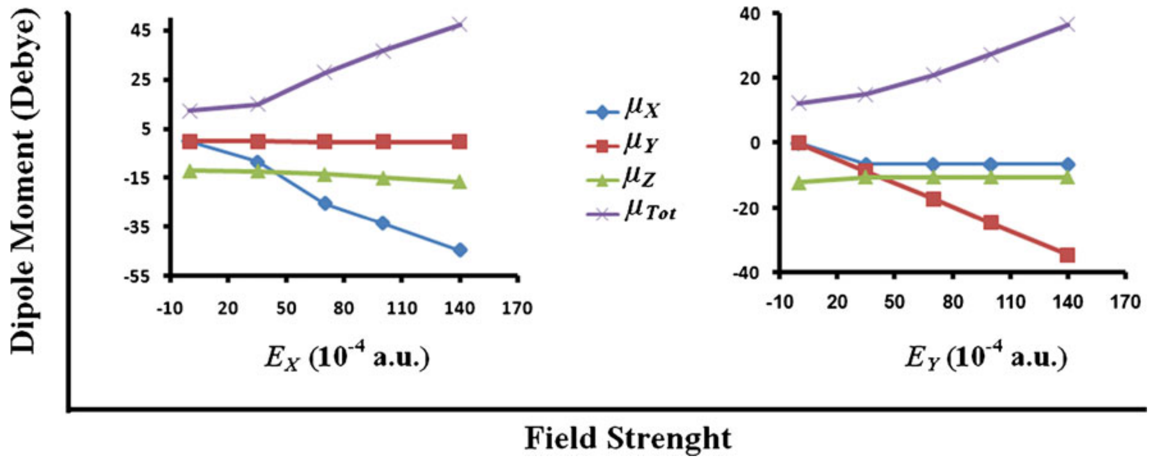

Fig. 4 Size of the electric dipole moment vector and its components (in Debye) at different applied parallel and transverse electric field strengths

Table 4 Natural bond orbital charges (NBO) at different applied parallel and transverse electric field strengths on the Al atoms

Atom	(6,0) *zigzag* AlNNT									
	X					Y				
	0	35	70	100	140	0	35	70	100	140
Al1	1.675	1.672	1.679	1.680	1.682	1.675	1.675	1.673	1.668	1.664
Al2	1.676	1.679	1.676	1.675	1.675	1.676	1.675	1.675	1.676	1.677
Al3	1.676	1.679	1.673	1.670	1.666	1.676	1.679	1.684	1.687	1.692
Al4	1.675	1.672	1.672	1.673	1.673	1.675	1.675	1.672	1.670	1.667
Al5	1.676	1.675	1.673	1.671	1.669	1.676	1.674	1.673	1.671	1.668
Al6	1.676	1.675	1.674	1.671	1.668	1.676	1.674	1.672	1.674	1.676
Al7	1.910	1.908	1.901	1.896	1.889	1.910	1.909	1.908	1.908	1.907
Al8	1.910	1.904	1.907	1.906	1.904	1.910	1.906	1.900	1.894	1.887
Al9	1.910	1.908	1.914	1.915	1.916	1.910	1.906	1.902	1.899	1.894
Al10	1.910	1.912	1.916	1.917	1.919	1.910	1.911	1.912	1.913	1.915
Al11	1.910	1.914	1.911	1.911	1.912	1.910	1.914	1.917	1.919	1.921
Al12	1.910	1.912	1.903	1.900	1.895	1.910	1.913	1.916	1.917	1.919
Al13	1.927	1.927	1.921	1.918	1.914	1.927	1.928	1.929	1.929	1.930
Al14	1.927	1.924	1.923	1.920	1.917	1.927	1.925	1.923	1.921	1.918
Al15	1.927	1.924	1.928	1.928	1.928	1.927	1.924	1.920	1.917	1.913
Al16	1.927	1.927	1.930	1.932	1.933	1.927	1.926	1.925	1.924	1.923
Al17	1.927	1.929	1.930	1.931	1.931	1.927	1.929	1.931	1.932	1.933
Al18	1.927	1.929	1.926	1.924	1.923	1.927	1.930	1.932	1.933	1.934
Al19	1.917	1.915	1.912	1.909	1.905	1.917	1.917	1.915	1.914	1.913
Al20	1.917	1.914	1.916	1.915	1.914	1.917	1.914	1.910	1.906	1.901
Al21	1.917	1.915	1.921	1.922	1.923	1.917	1.915	1.912	1.909	1.905
Al22	1.917	1.919	1.922	1.923	1.924	1.917	1.918	1.918	1.919	1.919
Al23	1.917	1.920	1.919	1.919	1.920	1.917	1.919	1.922	1.923	1.923
Al24	1.917	1.919	1.913	1.911	1.909	1.917	1.919	1.921	1.922	1.923
Al25	1.900	1.900	1.895	1.892	1.888	1.900	1.902	1.904	1.905	1.907
Al26	1.900	1.895	1.897	1.896	1.894	1.900	1.896	1.892	1.888	1.882
Al27	1.900	1.895	1.908	1.911	1.915	1.900	1.894	1.887	1.881	1.873
Al28	1.900	1.900	1.914	1.919	1.926	1.900	1.899	1.897	1.896	1.894
Al29	1.900	1.905	1.912	1.917	1.923	1.900	1.904	1.908	1.911	1.915
Al30	1.900	1.905	1.903	1.904	1.905	1.900	1.906	1.910	1.914	1.918

Table 5 Natural bond orbital charges (NBO) at different applied parallel and transverse electric field strengths on the N atoms

Atom	(6,0) *zigzag* AlNNT									
	X					Y				
	0	35	70	100	140	0	35	70	100	140
N1	−1.925	−1.923	−1.919	−1.916	−1.911	−1.925	−1.924	−1.923	−1.922	−1.920
N2	−1.925	−1.924	−1.922	−1.920	−1.918	−1.925	−1.923	−1.920	−1.918	−1.914
N3	−1.925	−1.923	−1.926	−1.926	−1.926	−1.925	−1.923	−1.921	−1.920	−1.917
N4	−1.925	−1.925	−1.928	−1.929	−1.931	−1.925	−1.925	−1.925	−1.924	−1.923
N5	−1.925	−1.928	−1.924	−1.923	−1.922	−1.925	−1.927	−1.929	−1.931	−1.933
N6	−1.925	−1.925	−1.920	−1.918	−1.914	−1.925	−1.927	−1.928	−1.928	−1.929
N7	−1.926	−1.926	−1.918	−1.914	−1.908	−1.926	−1.927	−1.928	−1.929	−1.930
N8	−1.926	−1.922	−1.920	−1.917	−1.913	−1.926	−1.924	−1.920	−1.917	−1.914
N9	−1.926	−1.922	−1.927	−1.927	−1.927	−1.926	−1.922	−1.917	−1.912	−1.906
N10	−1.925	−1.926	−1.932	−1.934	−1.936	−1.925	−1.925	−1.924	−1.922	−1.921
N11	−1.662	−1.930	−1.930	−1.932	−1.933	−1.662	−1.929	−1.931	−1.933	−1.935
N12	−1.926	−1.930	−1.923	−1.922	−1.921	−1.926	−1.930	−1.933	−1.935	−1.938
N13	−1.924	−1.921	−1.916	−1.912	−1.906	−1.924	−1.923	−1.922	−1.921	−1.920
N14	−1.924	−1.919	−1.921	−1.920	−1.919	−1.924	−1.919	−1.914	−1.910	−1.904
N15	−1.924	−1.922	−1.928	−1.930	−1.932	−1.924	−1.920	−1.917	−1.913	−1.909
N16	−1.924	−1.926	−1.930	−1.932	−1.934	−1.924	−1.925	−1.925	−1.926	−1.927
N17	−1.924	−1.930	−1.926	−1.926	−1.927	−1.924	−1.928	−1.931	−1.933	−1.936
N18	−1.924	−1.926	−1.918	−1.916	−1.912	−1.924	−1.927	−1.930	−1.931	−1.934
N19	−1.927	−1.927	−1.919	−1.916	−1.910	−1.927	−1.928	−1.930	−1.931	−1.932
N20	−1.927	−1.922	−1.922	−1.919	−1.916	−1.927	−1.924	−1.920	−1.916	−1.912
N21	−1.927	−1.922	−1.930	−1.931	−1.932	−1.927	−1.922	−1.916	−1.910	−1.902
N22	−1.927	−1.927	−1.935	−1.938	−1.942	−1.927	−1.926	−1.924	−1.923	−1.921
N23	−1.927	−1.931	−1.934	−1.936	−1.939	−1.927	−1.931	−1.933	−1.936	−1.938
N24	−1.927	−1.931	−1.926	−1.925	−1.925	−1.927	−1.931	−1.935	−1.938	−1.941
N25	−1.662	−1.659	−1.655	−1.652	−1.647	−1.662	−1.660	−1.659	−1.658	−1.657
N26	−1.662	−1.655	−1.663	−1.664	−1.664	−1.662	−1.656	−1.649	−1.659	−1.634
N27	−1.662	−1.659	−1.673	−1.678	−1.683	−1.662	−1.658	−1.653	−1.648	−1.642
N28	−1.662	−1.665	−1.676	−1.681	−1.688	−1.662	−1.664	−1.665	−1.666	−1.668
N29	−1.662	−1.668	−1.669	−1.672	−1.675	−1.662	−1.669	−1.674	−1.678	−1.684
N30	−1.662	−1.665	−1.659	−1.657	−1.655	−1.662	−1.667	−1.672	−1.675	−1.678

LUMO values for the applied perpendicular electric field is gradually decreased from −6.42 and −2.13 eV at the zero field strength (E_Y=0) to −3.54 and −0.39 eV at the field strength of 140×10^{-4} a.u. (E_Y=140) (see Table 8).

Dipole moment (μ)

When a nanotube is placed in external electric field, its atomic charge distribution are easily changed and the centers of the positive and negative charges of the nanotube change due to redistribution of the atomic charges consequently leads to the polarization of the nanotube and give it an induced electric dipole moment. As is evident from Table 3, values of the induced electric dipole moment (μ_{Tot}) vector obtained from these calculations increases linearly with increase in the applied external electric field strengths. Therefore, the electric dipole moment of a nanotube is an important property that characterizes information about its electronic and geometrical structure. The size and components of the electric dipoles moment (in Debye) for the nanotube at various applied parallel and transverse electric field strengths are shown in Fig. 4. μ_{Tol} and $|\mu_X|$ for the applied parallel electric field are gradually increased from 12.30 and 0.00 Debye at the zero field strength (E_X=0) to 47.42 and 44.40 Debye at the field strength of 140×10^{-4} a.u. (E_X=140) and μ_{Tol} and $|\mu_Y|$ for the applied transverse electric field are gradually increased from 12.30 and 0.00 Debye at the zero field strength (E_Y=0) to 36.55 and 34.43 Debye at the field strength of 140×10^{-4} a.u. (E_Y=140). These

Table 6 Differential values of natural bond orbital charges (NBO) at different applied parallel and transverse electric field strengths on the Al atoms

Atom	(6,0) *zigzag* AlNNT									
	X					Y				
	0	35	70	100	140	0	35	70	100	140
Al1	0.000	−0.003	0.004	0.005	0.007	0.000	0.000	−0.002	−0.007	−0.011
Al2	0.000	0.003	0.000	−0.001	−0.001	0.000	−0.001	−0.001	0.000	0.001
Al3	0.000	0.003	−0.003	−0.006	−0.010	0.000	0.003	0.008	0.011	0.016
Al4	0.000	−0.003	−0.003	−0.002	−0.002	0.000	0.000	−0.003	−0.005	−0.008
Al5	0.000	−0.001	−0.003	−0.005	−0.007	0.000	−0.002	−0.003	−0.005	−0.008
Al6	0.000	−0.001	−0.002	−0.005	−0.008	0.000	−0.002	−0.004	−0.002	0.000
Al7	0.000	−0.002	−0.009	−0.014	−0.021	0.000	−0.001	−0.002	−0.002	−0.003
Al8	0.000	−0.006	−0.003	−0.004	−0.006	0.000	−0.004	−0.010	−0.016	−0.023
Al9	0.000	−0.002	0.004	0.005	0.006	0.000	−0.004	−0.008	−0.011	−0.016
Al10	0.000	0.002	0.006	0.007	0.009	0.000	0.001	0.002	0.003	0.005
Al11	0.000	0.004	0.001	0.001	0.002	0.000	0.004	0.007	0.009	0.011
Al12	0.000	0.002	−0.007	−0.010	−0.015	0.000	0.003	0.006	0.007	0.009
Al13	0.000	0.000	−0.006	−0.009	−0.013	0.000	0.001	0.002	0.002	0.003
Al14	0.000	−0.003	−0.004	−0.007	−0.010	0.000	−0.002	−0.004	−0.006	−0.009
Al15	0.000	−0.003	0.001	0.001	0.001	0.000	−0.003	−0.007	−0.010	−0.014
Al16	0.000	0.000	0.003	0.005	0.006	0.000	−0.001	−0.002	−0.003	−0.004
Al17	0.000	0.002	0.003	0.004	0.004	0.000	0.002	0.004	0.005	0.006
Al18	0.000	0.002	−0.001	−0.003	−0.004	0.000	0.003	0.005	0.006	0.007
Al19	0.000	−0.002	−0.005	−0.008	−0.012	0.000	0.000	−0.002	−0.003	−0.004
Al20	0.000	−0.003	−0.001	−0.002	−0.003	0.000	−0.003	−0.007	−0.011	−0.016
Al21	0.000	−0.002	0.004	0.005	0.006	0.000	−0.002	−0.005	−0.008	−0.012
Al22	0.000	0.002	0.005	0.006	0.007	0.000	0.001	0.001	0.002	0.002
Al23	0.000	0.003	0.002	0.002	0.003	0.000	0.002	0.005	0.006	0.006
Al24	0.000	0.002	−0.004	−0.006	−0.008	0.000	0.002	0.004	0.005	0.006
Al25	0.000	0.000	−0.005	−0.008	−0.012	0.000	0.002	0.004	0.005	0.007
Al26	0.000	−0.005	−0.003	−0.004	−0.006	0.000	−0.004	−0.008	−0.012	−0.018
Al27	0.000	−0.005	0.008	0.011	0.015	0.000	−0.006	−0.013	−0.019	−0.027
Al28	0.000	0.000	0.014	0.019	0.026	0.000	−0.001	−0.003	−0.004	−0.006
Al29	0.000	0.005	0.012	0.017	0.023	0.000	0.004	0.008	0.011	0.015
Al30	0.000	0.005	0.003	0.004	0.005	0.000	0.006	0.010	0.014	0.018

results show that when the nanotube is exposed to external electric field, it has a much stronger interaction with the electrodes of the nano-electronic circuit.

Charge density distribution

As shown in the dipole moment section, because of applied external electric field strengths, the electronic charge distribution on atoms of the nanotube are changed and consequently, all charge-related molecular properties became different. Therefore, study of the electric field-dependent charge distribution that directly determined molecular behavior is important. In order to study the atomic charge distribution as a function of parallel and transverse electric field strengths (E_X and E_Y), the natural bond orbital charges (NBO) [15] have been calculated and summarized in Tables 4 and 5. Also, the significant changes in the NBO parameters for atoms of the AlNNT are summarized in Tables 6 and 7. The results presented in Table 6 indicate that large variations in Al atom's charge distribution at different parallel electric field strengths (E_X) are on Al28 and Al7 atoms, which increased and decreased gradually with field strengths, respectively. In Table 7, a similar trend in atomic charge variations are observed on N7 and N11 atoms. For the applied transverse electric field strengths (E_Y), large variations in Al atom's charge distribution are on Al30 and Al27 atoms, which increased and decreased gradually with field strengths and a similar trend in atomic charge variations are observed on N26 and N11 atoms. As is evident from Tables 6 and 7, the atomic charge variations

Table 7 Differential values of natural bond orbital charges (NBO) at different applied parallel and transverse electric field strengths on the N atoms

Atom	(6,0) *zigzag* AlNNT									
	X					Y				
	0	35	70	100	140	0	35	70	100	140
N1	0.000	0.002	0.006	0.009	0.014	0.000	0.001	0.002	0.003	0.005
N2	0.000	0.001	0.003	0.005	0.007	0.000	0.002	0.005	0.007	0.011
N3	0.000	0.002	−0.001	−0.001	−0.001	0.000	0.002	0.004	0.005	0.008
N4	0.000	0.000	−0.003	−0.004	−0.006	0.000	0.000	0.000	0.001	0.002
N5	0.000	−0.003	0.001	0.002	0.003	0.000	−0.002	−0.004	−0.006	−0.008
N6	0.000	0.000	0.005	0.007	0.011	0.000	−0.002	−0.003	−0.003	−0.004
N7	0.000	0.000	0.008	0.012	0.018	0.000	−0.001	−0.002	−0.003	−0.004
N8	0.000	0.004	0.006	0.009	0.013	0.000	0.002	0.006	0.009	0.012
N9	0.000	0.004	−0.001	−0.001	−0.001	0.000	0.004	0.009	0.014	0.020
N10	0.000	−0.001	−0.007	−0.009	−0.011	0.000	0.000	0.001	0.003	0.004
N11	0.000	−0.268	−0.268	−0.270	−0.271	0.000	−0.267	−0.269	−0.271	−0.273
N12	0.000	−0.004	0.003	0.004	0.005	0.000	−0.004	−0.007	−0.009	−0.012
N13	0.000	0.003	0.008	0.012	0.018	0.000	0.001	0.002	0.003	0.004
N14	0.000	0.005	0.003	0.004	0.005	0.000	0.005	0.010	0.014	0.020
N15	0.000	0.002	−0.004	−0.006	−0.008	0.000	0.004	0.007	0.011	0.015
N16	0.000	−0.002	−0.006	−0.008	−0.010	0.000	−0.001	−0.001	−0.002	−0.003
N17	0.000	−0.006	−0.002	−0.002	−0.003	0.000	−0.004	−0.007	−0.009	−0.012
N18	0.000	−0.002	0.006	0.008	0.012	0.000	−0.003	−0.006	−0.007	−0.010
N19	0.000	0.000	0.008	0.011	0.017	0.000	−0.001	−0.003	−0.004	−0.005
N20	0.000	0.005	0.005	0.008	0.011	0.000	0.003	0.007	0.011	0.015
N21	0.000	0.005	−0.003	−0.004	−0.005	0.000	0.005	0.011	0.017	0.025
N22	0.000	0.000	−0.008	−0.011	−0.015	0.000	0.001	0.003	0.004	0.006
N23	0.000	−0.004	−0.007	−0.009	−0.012	0.000	−0.004	−0.006	−0.009	−0.011
N24	0.000	−0.004	0.001	0.002	0.002	0.000	−0.004	−0.008	−0.011	−0.014
N25	0.000	0.003	0.007	0.010	0.015	0.000	0.002	0.003	0.004	0.005
N26	0.000	0.007	−0.001	−0.002	−0.002	0.000	0.006	0.013	0.003	0.028
N27	0.000	0.003	−0.011	−0.016	−0.021	0.000	0.004	0.009	0.014	0.020
N28	0.000	−0.003	−0.014	−0.019	−0.026	0.000	−0.002	−0.003	−0.004	−0.006
N29	0.000	−0.006	−0.007	−0.010	−0.013	0.000	−0.007	−0.012	−0.016	−0.022
N30	0.000	−0.003	0.003	0.005	0.007	0.000	−0.005	−0.010	−0.013	−0.016

obtained from these calculations increases with an increase in the applied external electric field strengths.

It is well known that atomic charges are arbitrarily-defined properties of questionable physical significance therefore, to help understand and predict nanotube interactions, the electrostatic potentials on surface of the (6,0) *zigzag* AlNNT have been computed at B3LYP exchange functional and 6-31 G* standard basis set. Also, the charge distribution can be explained by MEP calculations. The MEP is the potential generated by the charge distribution of the nanotube, which at an atomic site is defined as follows:

$$V(r) = \Sigma_A (Z_A / R_A - r) - \int \rho(r') dr' / |r' - r|, \quad (5)$$

where Z_A is the charge on nucleus A, located at R_A. The V(r) depends on whether the effects of the nuclei or the electrons are dominant at any point. The MEP has been used to explore the chemical properties of several materials [20, 21]. We computed the MEP surfaces for the (6,0) *zigzag* AlNNT in the different applied parallel, E_X, and perpendicular, E_Y, electric field strengths. As shown by the MEP plots in Fig. 5a, at zero fields (E_X=E_Y=0), the aluminum atoms are positively charged (blue colors) while the N atoms are relatively negatively charged (yellow or red colors) in Al–N bonds of the (6,0) *zigzag* AlNNT surface. It indicates that some charge is transferred from the Al atoms to the N ones resulting in an ionic bonding in AlNNT surface. On the other hand, as shown in Fig. 5, with an increase in the applied parallel and transverse electric field strengths (E_X and E_Y), the aluminum atoms color intensity is gradually decreased from blue

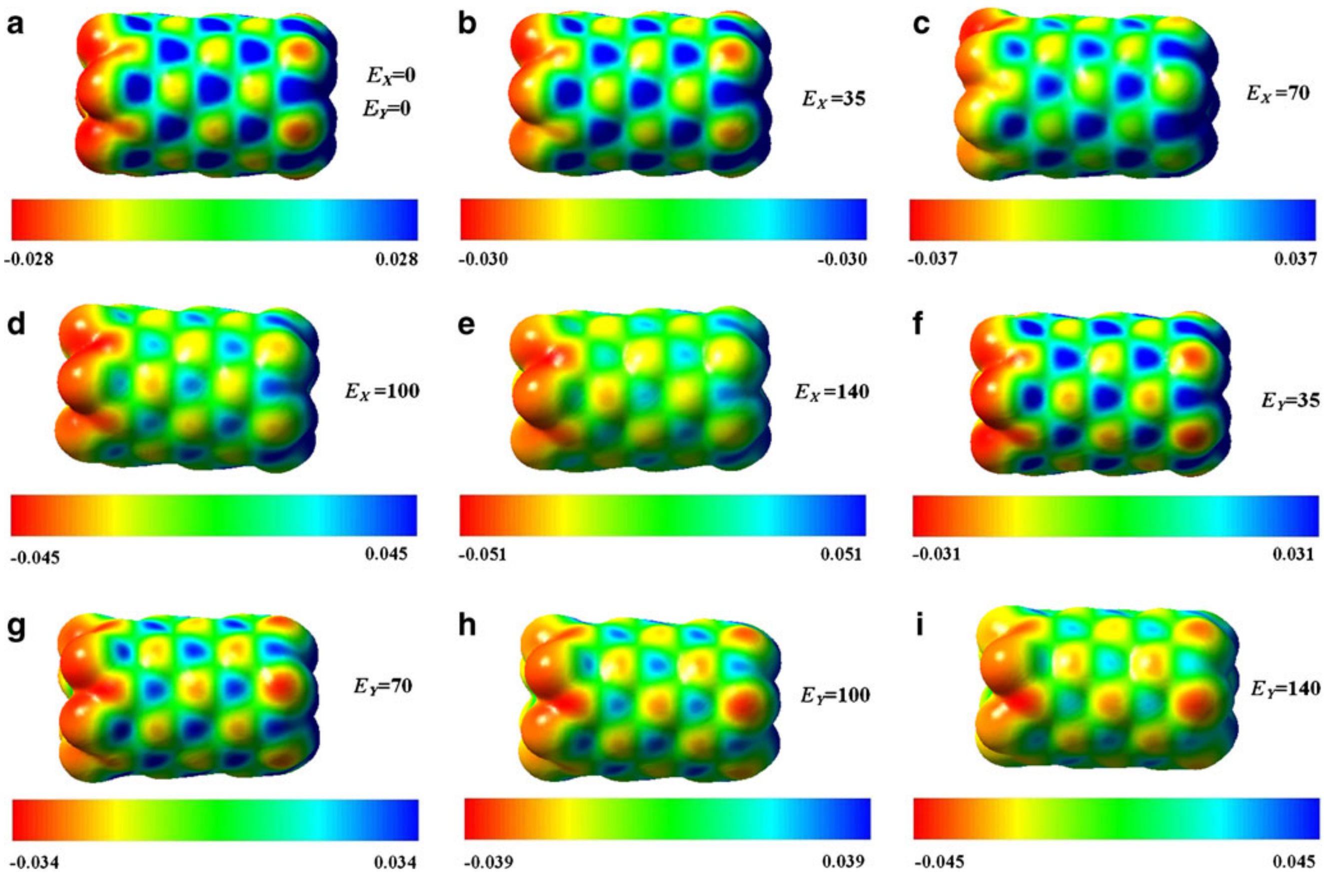

Fig. 5 Computed B3LYP/6-31G* electrostatic potentials on the molecular surfaces of the (6,0) *zigzag* AlNNT at different applied parallel and transverse electric field strengths. The surfaces are defined by the 0.0004 electrons/b3 contour of the electronic density. Color ranges are in a.u.

color to green color, therefore its atomic charge distributions are easily changed and the centers of the positive and negative charges of the nanotube change due to redistribution of the atomic charges by the external electric field.

Quantum molecular descriptors

The quantum molecular descriptors for the (6,0) *zigzag* AlNNT in the different applied parallel, E_X, and perpendicular, E_Y,

Table 8 Quantum molecular descriptors of the (6,0) *zigzag* AlNNT at different applied parallel and transverse electric field strengths

Property	(6,0) *zigzag* AlNNT									
	X					Y				
	0	35	70	100	140	0	35	70	100	140
E_{HOMO}/eV	−6.42	−6.33	−6.55	−6.52	−6.48	−6.42	−5.79	−5.06	−4.42	−3.54
E_{LUMO}/eV	−2.13	−2.16	−3.18	−3.78	−4.72	−2.13	−1.62	−1.16	−0.81	−0.39
[E_{LUMO} - E_{HOMO}]/eV	4.29	4.17	3.37	2.74	1.76	4.29	4.17	3.90	3.61	3.15
[I=− E_{HOMO}]/eV	6.42	6.33	6.55	6.52	6.48	6.42	5.79	5.06	4.42	3.54
[A=− E_{LUMO}]/eV	2.13	2.16	3.18	3.78	4.72	2.13	1.62	1.16	0.81	0.39
[$\eta=(I - A)/2$]/eV	2.14	2.08	1.68	1.37	0.88	2.14	2.08	1.95	1.80	1.58
[$\mu=-X=-(I+A)/2$]/eV	−4.28	−4.24	−4.86	−5.15	−5.60	−4.28	−3.70	−3.11	−2.62	−1.96
[$S=1/2\eta$]/eV^{-1}	0.23	0.24	0.30	0.36	0.57	0.23	0.24	0.26	0.28	0.32
[$\omega=\mu^2/2\ \eta$]/eV	4.28	4.32	7.03	9.68	17.82	4.28	3.29	2.48	1.91	1.22

I=ionization potential, A=electron affinity, η=Global hardness, S=Softness, μ=Chemical potential, X=electronegativity, and ω=electrophilicity electric field strengths are summarized in Table 8. We observe that with an increase in the applied external electric field strengths, the energy gap (E_{LUMO} - E_{HOMO}) of the nanotube decreased. This lowering of energy gap in the nanotube may be able to increase the reactivity of the nanotube. The results presented in Table 8 indicate that the ionization potential (I) for the applied parallel electric field do not have any well-defined trend from zero to 140×10^{-4} a.u. but in summary, the ionization potential (I) is increased from 6.42 at the zero field strength (E_X=0) to 6.48 at the field strength of 140×10^{-4} a.u. (E_X=140), also electron affinity (A) of the nanotube for the applied parallel electric field is gradually increased from 2.13 eV at the zero field strength (E_X=0) to 4.72 eV at the field strength of 140×10^{-4} a.u. (E_X=140). For the applied transverse electric field, the ionization potential (I) and electron affinity (A) of the nanotube are gradually decreased from 6.42 and 2.13 eV at the zero field strength (E_Y=0) to 3.54 and 0.39 eV at the field strength of 140×10^{-4} a.u. (E_Y=140). The chemical potential (μ) with increase of the applied parallel electric field strengths is gradually increased, whereas with an increase of the applied transverse electric field strengths are gradually decreased. The electrophilicity index (ω) is a measure of electrophilic power of a molecule. The electrophilicity of the nanotube with an increase of the applied parallel electric field strengths is strongly increased, whereas with an increase of the applied transverse electric field strengths are gradually decreased. These trends are in agreement with the changes in the ionization potential (I) and electron affinity (A) of the nanotube. In the nanotube, the ionization potential (I) and electron affinity (A) show a significant reverse trend with an increase of the applied transverse electric field (E_Y). The global hardness (η) of the nanotube at different external electric field strengths decreased, and consequently, the global softness (S) of the nanotube is increased. Decrease in global hardness and energy gap of the nanotube is due to external electric field strengths, and consequently, the stability of the nanotube is lowered and its reactivity increased. This increasing of the ionization potential (I), electron affinity (A), chemical potential (μ), electrophilicity (ω), and HOMO and LUMO in the nanotube with increase of the applied parallel electric field strengths shows that it has a much stronger interaction with the nanotube with respect to the transverse electric field strengths. The ionization potential (I), electron affinity (A), electronic chemical potential (μ), global hardness (η), electrophilicity index (ω), global softness (S), and electronegativity (χ) are all arbitrarily-defined quantities, not physical observables. Therefore, the values of the parameters are approximate.

Conclusions

We studied the structure and electronic properties including bond lengths, bond angles, length of tube, tip diameters, molecular volume, dipole moments (μ), energy gaps, energies, atomic charges, molecular orbital energies, electronic spatial extent (*ESE*), density of states, and quantum molecular descriptors on (6,0) zigzag AlNNT at different applied parallel and transverse electric field strengths by means of density functional theory (DFT) calculations. We compared all the parameters in the applied external electric field strengths. Analysis of the structural parameters indicates that both the geometry and electronic structure of AlNNT are sensitive to both the parallel and transverse electric fields, especially to the parallel electric fields. Therefore, the study of AlNNTs under influence of external electric field strengths is very important in relation to proposing or designing AlNNTs as a molecular scale device for nanoelectronic circuit. The length, tip diameters, electronic spatial extent, and molecular volume of the (6,0) *zigzag* AlNNT do not significantly change with increasing electric field strength and indicated that the nanotube is a stable molecule over the entire range of the applied electrical field strength.

References

1. Ijima S (1991) Nature 354:56–58
2. Derycke V, Martel R, Appenzeller J, Avouris Ph (2002) Appl Phys Lett 80:2773–2775
3. Liu C, Fan YY, Liu M, Cong HT, Cheng HM, Dresselhaus MS (1999) Science 286:1127–1129
4. Zurek B, Autschbach J (2004) J Am Chem Soc 126:13079–13088
5. Nojeh A, Lakatos GW, Peng S, Cho K, Pease RFW (2003) Nano Lett 3:1187–1190
6. Mirzaei M, Shif A, Hadipour NL (2008) Chem Phys Lett 461:246–248
7. Baei MT (2012) Monatsh Chem 143:545–549
8. Strite S, Morkoc H (1992) J Vac Sci Technol B 10:1237
9. Jain C, Willander M, Narayan J, van Overstraeten R (2000) J Appl Phys 87:965
10. Ruterana P, Albrecht M, Neugebauer J (2003) Nitride semiconductors: handbook on materials and devices. Wiley, New York
11. Khoo KH, Mazzoni MSC, Louie SG (2004) Phys Rev B 69:201401(R
12. Guo GY, Ishibashi S, Tamura T, Terakura K (2007) Phys Rev B 75:245403
13. Attaccalite C, Wirtz L, Marini A, Rubio A (2007) Phys Status Solidi B 244:4288–4292
14. Machado M, Azevedo S (2011) Eur Phys J B 81:121–125
15. Chattaraj PK, Sarkar U, Roy DR (2006) Chem Rev 106:2065–2091
16. Hazarika KK, Baruah NC, Deka RC (2009) Struct Chem 20:1079
17. Parr RG, Szentpaly L, Liu S (1999) J Am Chem Soc 121:1922–1924
18. Sabzyan H, Farmanzadeh D (2007) J Comput Chem 28:923
19. Schmidt M et al (1993) J Comput Chem 14:1347–1363
20. Politzer P, Lane P, Murray JS, Concha MC (2005) J Mol Model 11 (1):1
21. Peralta-Inga Z, Lane P, Murray JS, Boyd S, Grice ME, O'Connor CJ, Politzer P (2003) Nano Letters 3(1):21–28